Structure and photoinduced structural changes in a-As_2S_3 films: A study by differential anomalous x-ray scattering

Weiqing Zhou,* D. E. Sayers, and M. A. Paesler
Department of Physics, North Carolina State University, Raleigh, North Carolina 27695

B. Bouchet-Fabre, Q. Ma, and D. Raoux
Laboratoire pour l'Utilisation du Rayonnement Electromagnétique (LURE), Bâtiment 209D, Universite de Paris—Sud, 91405 Orsay CEDEX, France

(Received 10 March 1992)

Differential anomalous x-ray-scattering experiments were carried out on two samples, annealed and photodarkened a-As_2S_3 films of 4 μm in thickness. Two x-ray energies were chosen. One is 11 859 eV, just below the arsenic K edge; the other is 11 700 eV, below the edge by 167 eV. The study of the structure and photoinduced reversible structural changes in the a-As_2S_3 films show that the first sharp diffraction peak (FSDP) is related to intermediate-range correlations. These correlations extend as far as 7.0 Å. Beyond 7.0 Å, however, the structure in radial distribution function tends to the average atomic density. The FSDP is dominated by the arsenic-related atomic correlations, especially As-As atomic correlation. After photodarkening, the structure overall in both the short and intermediate ranges moves to a more disordered state. The photoinduced structural changes involve changes of the As-As atomic pair correlation in the intermediate range as illustrated by the comparisons of the changes between the annealed and photodarkened a-As_2S_3 films in the FSDP's and the differential structure factors.

I. INTRODUCTION

Amorphous (a-) As_2S_3 solid does not possess long-range order (LRO) as does its crystalline partner, c-As_2S_3, or orpiment. Studies by Raman, NMR, infrared spectroscopies, and other techniques showed that amorphous (or glassy) and crystalline As_2S_3 have a similar local structure[1–5] or short-range order (SRO), which includes chemical ordering as well as bond lengths and bond angles for nearest neighbors. Studies have shown that the structure in the intermediate regime between these extremes of SRO and LRO is not totally random in a-As_2S_3. The material possesses certain so-called intermediate-range order (IRO). IRO is currently one of the most controversial aspects of the structure of amorphous solids. Some of the strongest evidence for the existence of IRO is the presence of the so-called "first sharp diffraction peak (FSDP); in the x-ray[6–9] and neutron,[10–12] scattering intensities in a-As_2S_3, as well as in a variety of other amorphous solids, such as in amorphous[13] and liquid[14] $GeSe_2$. To understand the structure in both SRO and IRO, a variety of experimental techniques, such as x-ray scattering,[6–9] Raman scattering,[15,16] and their dependences on temperature, pressure, kinetics, etc., and computer modeling have been employed.

A unique phenomenon which exists in many chalcogenide materials and their alloys is the photoinduced structural change. This change can be irreversible or reversible.[7] In this study, we focus on the reversible photoinduced structural changes. The reversible photoinduced structural change involves photodarkening (a red-shift in optical absorption gap),[18] photodilation,[19,20] changes in bond statistics,[21–23] glass transition temperature,[24] microhardness[25] and optical anisotropy effects.[26–29] The microscopic mechanism of photodarkening associated with photoinduced structural changes in chalcogenide glasses has been studied for many years. To extract physical information about these changes in atomic, electronic, and magnetic properties and their dependences on temperature, composition, pressure, and kinetics, various experimental techniques have been employed. These include x-ray and neutron scattering,[18,30] x-ray-absorption spectroscopy,[22,23,31] electron spin resonance,[32–34] nuclear quadrupole resonance,[35,36] Mössbauer spectroscopy,[37–39] Raman,[15,21] and infrared spectroscopies.[36,40]

To further understand the structure and photoinduced structural changes, especially in the realm of the IRO, in this paper we present a study of a-As_2S_3 using differential anomalous x-ray scattering (DAXS). Like x-ray-absorption fine-structure (XAFS), DAXS can also provide species-specific structural information for a material containing more than one atomic species. Combined with EXAFS, detailed information about the SRO in complex amorphous materials can be obtained, and this information can be extended to IRO about specific species. In Sec. II, we discuss sample preparation and characterization. In Sec. III, we briefly describe the experiment and theory of DAXS and the methods of data analysis. In Sec. IV, we discuss the results in three subsections, viz., the total structural approach, the differential approach, and the first sharp diffraction peak. Finally, in Sec. V, we present the conclusions.

II. SAMPLE PREPARATION AND CHARACTERIZATION

The as-deposited a-As_2S_3 films were prepared by evaporating bulk glass As_2S_3 (of purity 99.99% manufac-

tured by CERAC) in a diffusion-pumped and cold-trapped system. The deposition rates for the samples used are about 20 Å per second. The vacuum pressure during evaporation was less than 10^{-6} torr. The substrate temperature was room temperature. The substrate materials chosen depend on the characterizations to be made; e.g., glass substrates for the optical transmission as well as Raman-scattering spectroscopies, Kapton substrates for XAFS, and c-Si (100) wafer substrates for DAXS.

After deposition, the thin films were moved into an annealing chamber. Annealing was at 445 K for 1 in a flow of high-purity argon gas in the dark. Then, through a slow cooling cycle, the temperature of the samples was brought back to room temperature. For the study of the light-soaking effect, the annealed samples were subsequently exposed to an Ar laser beam (488 nm and 100 nW) for more than 20 min at 77 K in liquid nitrogen to avoid photo-oxidation on the surfaces.

The composition of the annealed As_xS_{1-x} film as determined by x-ray-absorption spectroscopy is at $x=0.40$ with the error bar of 0.02. We also examined the structure of our films by using Raman spectroscopy. The Raman spectra of the a-As_2S_3 annealed films were essentially identical to those measured in the bulk glass.[41–43] The films were also measured using an optical transmission spectrometer to characterize the shifts of optical absorption edge as well as the changes in thickness. Taking the values of coefficient at $\alpha=5\times10^3$ cm^{-1}, the optical edge shift is $\Delta E=0.07$ eV or $\Delta E/E=2.8\%$ for a-As_2S_3, which are in the range of the published results.[36] From the periodic fluctuations of the transmission data, we also can estimate the thickness of the samples. The a-As_2S_3 films show an increase in thickness (assuming changes of the index of refraction n can be neglected) after photodarkening by 0.8%. In brief, the a-As_2S_3 films prepared for the DAXS study show in their Raman spectra, their optical edge shifts, and their changes in thickness a good agreement with reported results.

III. DIFFERENTIAL ANOMALOUS X-RAY SCATTERING

A. Theory

When studying amorphous alloys with DAXS, one generally assumes that correlations are equally likely to occur in any direction. The resulting x-ray-scattering intensity can be written as

$$I_a(q,E)=\langle f(q,E)^2\rangle-\langle F(q,E)\rangle^2+\langle f(q,E)\rangle^2 S(q)\ , \tag{1}$$

where, for a binary sample,

$$\langle f(q,E)^2\rangle=\sum_{i=1}^{2} c_i|f_i(q,E)|^2$$

and

$$\langle f(q,E)\rangle^2=\left[\sum_{i=1}^{2} c_i f_i(q,E)\right]^2 .$$

Here c_i is the atomic fraction of species i. The atomic scattering factor, or coherent cross section, for each species is expressed in electron units as

$$f(q,E)=f_0(q)+f'(q,E)+if''(q,E)\ , \tag{2}$$

where $q=|\mathbf{q}|=(4\pi\sin\theta)/\lambda$ is the magnitude of the scattering vector determined by the scattering angle 2θ and the x-ray wavelength λ, and E is the photon energy. The energy-independent scattering factor $f_0(q)$ used in this work was obtained from parametrized results of calculations by Cromer and Mann.[44] The anomalous scattering factors (AFS's) $f'(q,E)$ and $f''(q,E)$ become significant when the photon energies are near the characteristic absorption edge energies of the atomic species in the sample. f'' represents the absorption contribution to the scattering factor, which was measured by an x-ray-absorption experiment over a broad energy range near the arsenic K edge of an a-As_2S_3 film. f' was calculated from f'' via a Kramers-Kronig dispersion relation.[45] $f'(E)$ and $f''(E)$ for a-As_2S_3 are shown in Fig. 1. At the x-ray energies used in this study of 11 859 eV (-8 eV below the absorption edge) and 11 700 eV (-167 eV below the edge), f' is -8 and -4 electrons, respectively.

The total structure factor $S(q)$ can be expressed as a linear combination of the partial structures factors (PSF) $S_{ij}(q)$ weighted by weighting factors $W_{ij}(q,E)$,

$$S(q)=\sum_{i=1}^{2}\sum_{j=1}^{2} W_{ij}(q,E)S_{ij}(q)\ , \tag{3}$$

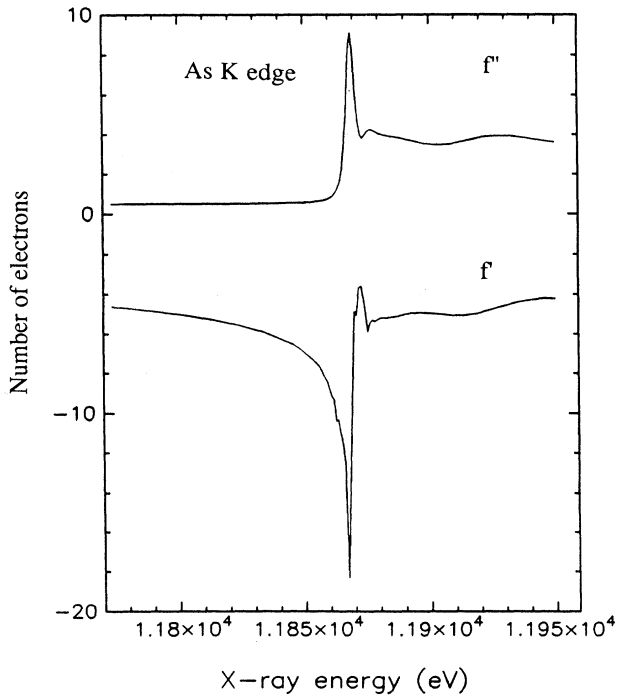

FIG. 1. $f'(E)$ and $f''(E)$ of a-As_2S_3 and As K edge energy, 11 867 eV, plotted vs x-ray energy.

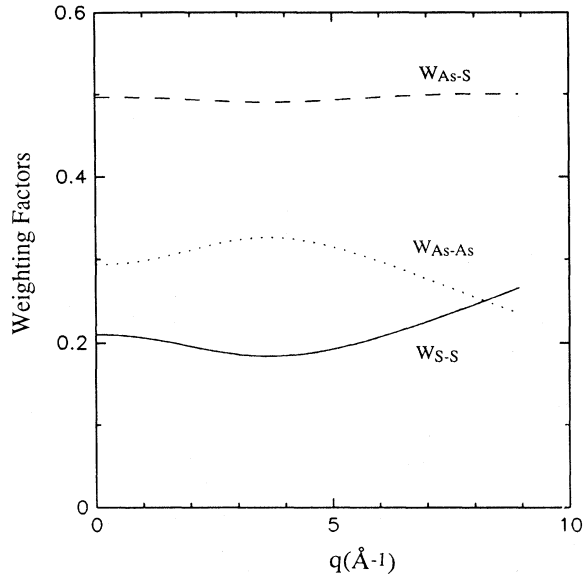

FIG. 2. The weighting factors of As-As, As-S, and S-S atomic pairs vs q (in Å^{-1}) at energy 11 700 eV.

where

$$W_{ij}(q,E)=c_i c_j \frac{f_i(q,E)f_j(q,E)}{\langle f(q,E)\rangle^2} \ . \tag{4}$$

ρ_0 is the average atomic density and $g_{ij}(r)$ is the partial reduced radial distribution function. Figures 2 and 3 show the weighting factors of As-As, As-S, and S-S atomic pairs at two different energies, 11 700 and 11 859 eV, respectively, where we can see that the partial structure factors play a different role with the change of energy.

A Fourier transform of the reduced total structure factor $q(S(q)-1)$ gives the reduced distribution function which is expressed as

$$4\pi r\rho_0[g(r)-1]=\left[\frac{2}{\pi}\right]\int q[S(q)-1]\sin(qr)dq \ , \tag{5}$$

where $4\pi r^2\rho_0 g(r)$ is the distribution function.

In use of the anomalous scattering effect at a given species edge proposed by Shevchik[46,47] and first implemented by Fuoss *et al.*[48] one uses the difference

$$I(q,E_1)-I(q,E_2) =\Delta_A[\langle f^2\rangle-\langle f\rangle^2]+\Delta_A[\langle f\rangle^2]\Delta S(q) \ , \tag{6}$$

where $\Delta_A[\ ]$ indicates the difference between energies E_1 and E_2 of the quantity in square brackets. The energies E_1 and E_2 are chosen so that only the As atom's scattering factor changes, thus Eq. (6) is sensitive only to correlation involving As (i.e., As-As and As-S). The differential structure factor $\Delta S(q)$ for a binary material is defined as

$$\Delta S(q)=\sum_{i=1}^{2}\sum_{j=1}^{2} W_{ij}(q,E_1,E_2)S_{ij}(q) \ , \tag{7}$$

where the weighting factors are

$$W_{ij}(q,E_1,E_2)=c_i c_j \frac{\Delta_A[f_i f_j]}{\Delta_A[\langle f\rangle^2]} \ . \tag{8}$$

In the case of a-As_2S_3, the differential weighting factors from two different energies (11 859 and 11 700 eV) for As-As, As-S, and S-S atomic pairs are shown in Fig. 4. As we can see, the arsenic-related weighting factor is still finite, while the S-S weighting factor approaches zero. This thus removes the S-S partial structure factor in Eq. (8) and gives the arsenic atomic environment.

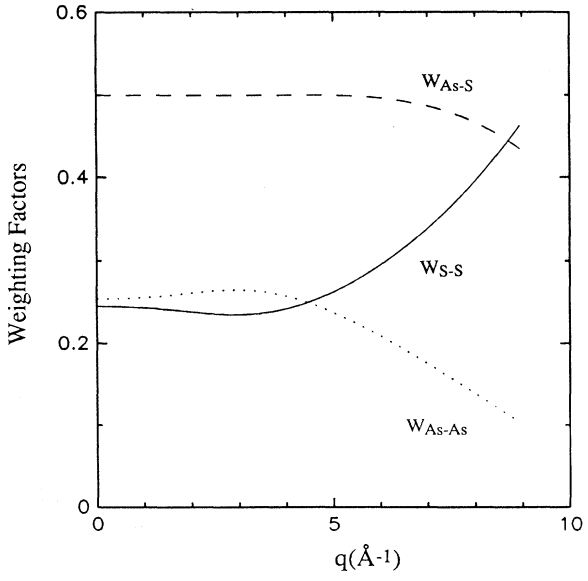

FIG. 3. The weighting factors of As-As, As-S, and S-S atomic pairs vs q (in Å^{-1}) at energy 11 859 eV.

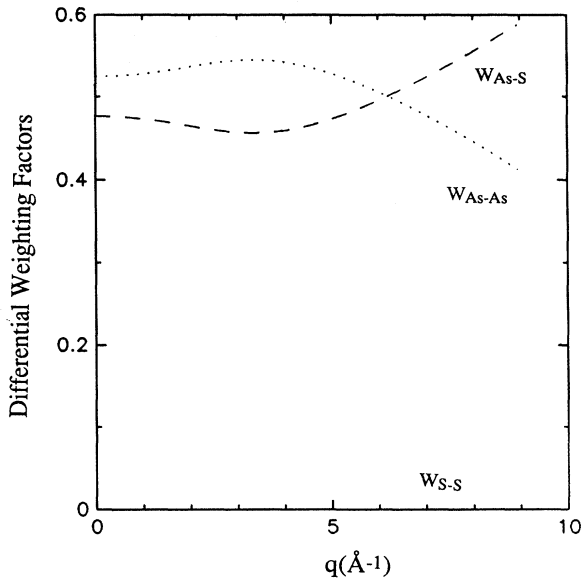

FIG. 4. The differential weighting factors vs q (in Å^{-1}) at energies, 11 859 and 11 700 eV, for As-As, As-S, and S-S atomic pairs.

B. Experiment

The DAXS experiments were carried out at the Wiggler beam line at LURE-DCI, in France. Figure 5 is the schematic drawing of the experimental apparatus. The x-ray beam from the wiggler magnet ($W1$) on the DCI storage ring passes through a beryllium window, is confined by a two-dimensional adjustable slit, S_1, and then enters the double-crystal monochromator which consists of two independent silicon (220) crystals. The temperature of the crystals was controlled at 12 °C. The beam out of the monochromator was partially reflected by Kapton tape to a photomultiplier (PM) to take into account the decay of the beam, and finally impinges on the sample. The slits S_1 and S_4 restrict the beam size which, in turn, control the band pass of the photon energy. Slits S_2 and S_3 were used to remove stray light to improve the signal-to-noise level. The sample is mounted on a two circle goniometers, which can separately control rotations of the sample and the detector in the vertical plane. The scattering pattern was recorded with a step by step method using a fixed time interval of 15 s per step. The step size was 0.05 Å^{-1} in q.

The detector active area is formed by 12 parallel Si:Li plates. Each plate is 20 mm long and 2 mm high. The interval between plates is 2 mm.[49] Each plate is used as an independent detector. A radial slit system is used to reduce spurious signals (mostly air scattering). The photon-activated charges are collected in 12 independent charge preamplifiers. The output voltage signals are processed independently in 12 amplifiers which produce a pulse for each event of height proportional to the photon energy. The energy resolution is better than 260 eV at the iron K edge, which is sufficient to discriminate against the $K\alpha$, but not the $K\beta$ fluorescence in the experimental spectra. To experimentally obtain the ratio between fluorescence $K\alpha$ and $K\beta$, a measurement at x-ray energy far above the arsenic K edge was made to sufficiently separate $K\beta$ from the coherent part of the signal. The ratio $K\beta/K\alpha$ was found to be 0.169. During the experimental manipulations, the multiwindow setup in the multichannel analyzers allowed us to simultaneously collect the scattering data, which was mixed with fluorescence $K\beta$ and Compton scattering, and fluorescence $K\alpha$. The advantage of this setup was to let one get fluorescence $K\beta$ from the experimental data of fluorescence $K\alpha$ which was multiplied by the ratio $K\beta/K\alpha$ as given above. And then one can subtract this fluorescence $K\beta$ from the scattering data. Under the conditions used in this experiment, the linearity of the counting rate is found to have no deviation up to 3000 counts per s (cps) in each detector. The rate decreases by less than 7% at 5000 cps. The maximum rates in the range of the data we used did not exceed 3000 cps. The amplifier outputs are sent to a multiplexer system which includes a fast analog-to-digital converter (ADC). The ADC converts the signals over a range of 512 channels which can be set up to 16 regions and used as a multichannel analyzer for an incremental memory.

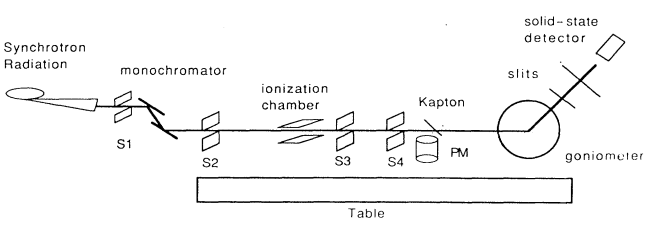

FIG. 5. Schematic drawing of the differential anomalous x-ray-scattering experimental aparatus.

For the As_2S_3 thin films, 4 μm in total thickness, the measured signals at the detector include not only the elastic scattering, but are also affected by the substrate, air scattering, fluorescence, and Compton scattering. Furthermore, the signal is also distorted by absorption and geometrical factors. In order to eliminate a great part of the substrate signal, a grazing incidence geometry was used where the angle θ_0 was fixed at 3°. The data correction procedures[5] include (1) normalization by the intensity of the incident beam which allows one to remove the time instability of the incident x-ray beam; (2) the geometry absorption correction; (3) the removal effects of the silicon substrate; (4) the polarization correction; (5) the interactive volume correction; (6) subtraction of fluorescence $K\beta$; (7) normalization to a per electron scale;[51,52] and (8) subtraction of the Compton scattering.

IV. RESULTS AND DISCUSSIONS

This section includes three subsections. The first contains the total structural approach presenting the data of two samples (annealed and photodarkened a-As_2S_3), measured at two different x-ray energies, (11 859 eV near the arsenic K edge, and 11 700 eV below the edge by 167 eV). The second subsection includes the differential results, and the third contains a discussion of the first sharp diffraction peak.

A. Total structural factors

Two samples, both annealed and photodarkened, were measured consecutively at two energies, 11 859 and 11 700 eV, respectively. Table I lists all the values of f' and f'' of arsenic, sulfur, and silicon atoms at arsenic $K\alpha$ (10 530 eV), $K\beta$ (11 722 eV), and the two measured x-ray energies (11 700 and 11 859 eV). After treating the data as discussed in Sec. III and removing the unphysical oscillations for $0 \le r \le 1.8$ Å (which are related to slow variance of the background distortions with scattering angle and inversing Fourier transform back to q space), one obtains the coherent scattering intensities as shown in Fig. 6 for the both annealed and photodarkened samples. The

TABLE I. f' and f'' values (electron units) of As, S, and Si atoms at the energies used in this experiment.

Energy (eV)	f' (As)	f'' (As)	f' (S)	f'' (S)	f' (Si)	f'' (Si)
11 859	−8.20	0.674	0.238	0.339	0.170	0.198
11 700	−4.20	0.500	0.234	0.331	0.166	0.193
11 722	−4.24	0.500	0.234	0.332	0.166	0.193
10 530	−2.07	0.617	0.204	0.269	0.140	0.156

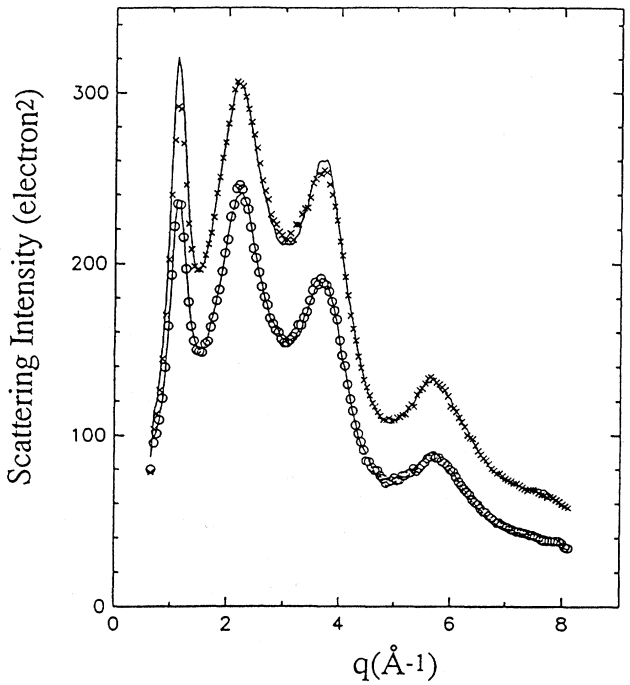

FIG. 6. Elastic scattering intensity (electron^2) vs q. The upper two curves are for a scattering energy of 11 700 eV and the lower two curves for 11 859 eV. The solid lines are the a-As_2S_3 annealed film and the crossed and circled lines are the photodarkened film.

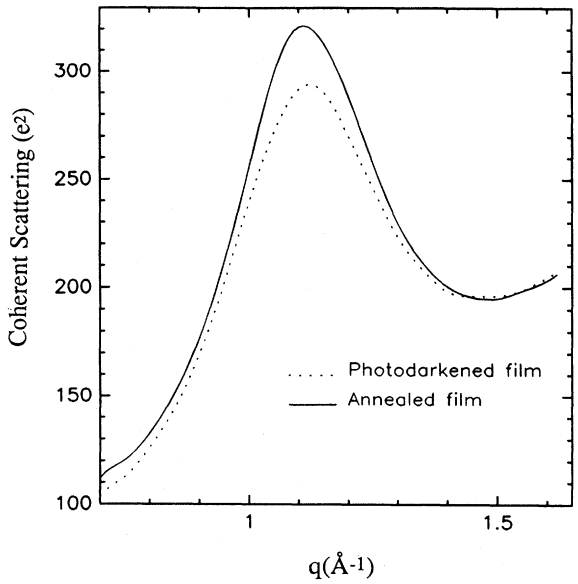

FIG. 7. A local enlargement of Fig. 6 around the FSDP for the data taken at 11 700 eV. The solid line is the annealed a-As_2S_3 film and the dotted line is the photodarkened film.

uppermost curves were measured at 11 700 eV, while the lower curves were measured at 11 859 eV. The solid curves are the annealed film while the dotted curves are the photodarkened film. Both figures show overall excellent matches between the annealed and photodarkened films from low to high q. However, clear differences between the annealed and photodarkened films, especially at 11 700 eV in Fig. 6, can be observed. Enlargements of the region from 1.25 to 1.8 Å^{-1} are shown in Figs. 7 and 8 at energies at 11 700 and 11 859 eV, respectively. Figure 7 shows that the intensity of the first sharp diffraction peak at $q=1.12$ Å^{-1} is lowered from 320 electron^2 in the annealed film to 290 electron^2 in the photodarkened film. The peak is also slightly shifted from $q=1.12$ to 1.13 Å^{-1}. The changes of both the intensity and the shift were first reported by Tanaka.[53] However, our results show the minimum at $q=1.55$ Å^{-1} does not increase as given by Tanaka,[53] but is roughly unchanged. We believe this is because our data are over a longer range in k which allows for a better normalization procedure. The differences between the annealed and photodarkened films for both lower and higher q values indicate photoinduced structural changes involve IRO as well as SRO. However, the scattering intensities in the annealed and photodarkened films at an x-ray energy of 11 859 eV in Fig. 8 do not show as significant a change as they do at 11 700 eV in Fig. 7.

The only difference between the x-ray scattering at the two energies is the weighting factors for each atomic pair correlation which change as shown in Figs. 2 and 3. In the regions of the FSDP, the As-S weight factor, $W_{\text{As-S}}$, is essentially unchanged between 11 700 and 11 859 eV. The As-As weight factor, $W_{\text{As-As}}$, on the other hand, changes by approximately 0.1 between these two energies. Thus, the photoinduced changes in the FSDP at 11 700 eV (Fig. 7) coupled with the lack of any such changes at 11 859 eV (Fig. 8) suggest that the modifications in structure resulting from photoirradiation

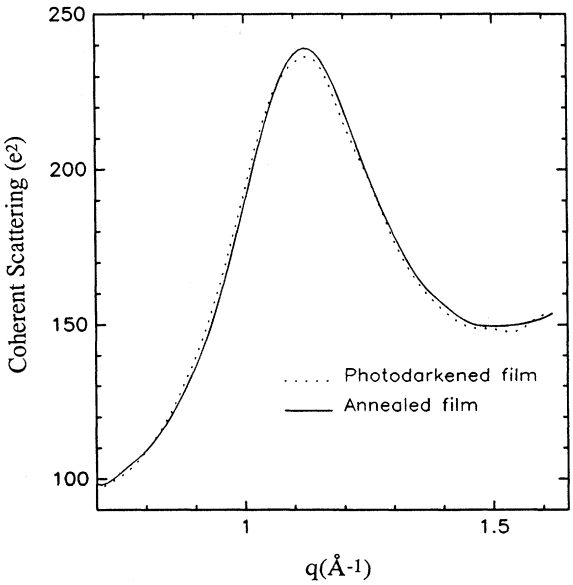

FIG. 8. A local enlargement of Fig. 6 around the FSDP for the data taken at 11 859 eV. The solid line is the a-As_2S_3 annealed film and the dotted line is the photodarkened film.

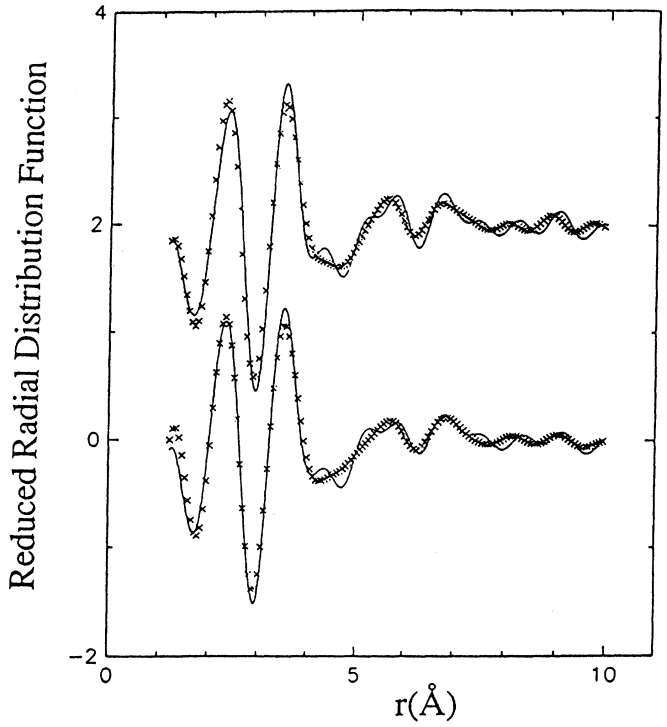

FIG. 9. The reduced radial distribution functions of the data in Fig. 6 vs r. The upper two curves were taken at x-ray energy 11 859 eV; the lower two curves were taken at 11 700 eV. The solid lines are for the annealed film, and the crossed lines for the photodarkened film. The transform was taken over the range $q=0.65-8.0$ Å^{-1}.

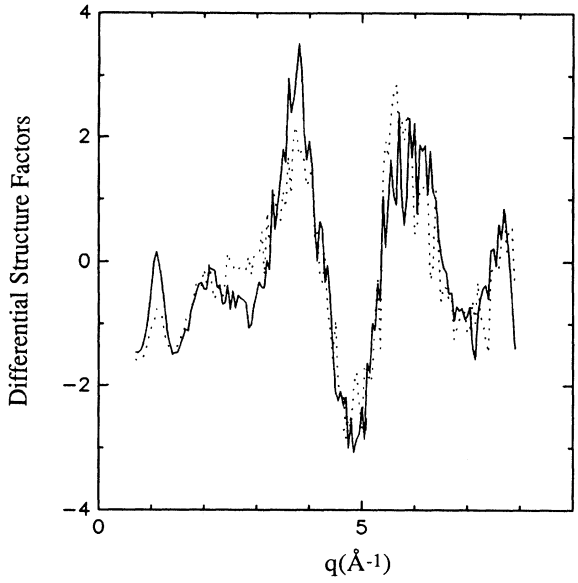

FIG. 10. The differential structural factors. The solid line is the annealed a-As_2S_3 film, and the dotted line is the photodarkened film.

are mainly associated with As-As atomic pair correlations and not with As-S correlations. (Any association with S-S correlations can even more clearly be ruled out with differential scattering, as is shown in the next subsection.) Whether photodarkening itself is mainly related to As-As correlations or not, these results suggest that such correlation play a very important role in the photodarkening process.

Using Eq. (1), we can get the total scattering structure factors. Converting the data to the reduced scattering structure factors $q[S(q)-1]$, and then taking Fourier transforms over a range from $q=0.65$ to 8.0 Å-1, we can get the total reduced radial distribution functions as shown in Fig. 9 at x-ray energies of 11 700 (two top curves) and 11 859 eV (two bottom curves), respectively. The solid curves are the annealed film and the crossed curves are the photodarkened film. Comparing the two curves at the same energies in Fig. 9, we can see a slight difference where the curves of the photodarkened film shows a lower and broader amplitude which also indicate the structure after photodarkening changes to a more disordered state in both the SRO and IRO.

B. Differential approach

As suggested above, the As-As atomic pair correlation is very important in photodarkening. To further examine this assertion, we use the differential approach as discussed in Sec. III. Figure 10 shows the differential structure factors between two energies, 11 700 and 11 859 eV. The solid line is the annealed a-As_2S_3 film, while the dotted line is the photodarkened film. As shown in Fig. 4, the differential spectra remove the S-S atomic pair correlations, and only include the As-As and As-S correlations, which give the environment of arsenic atoms. The fact that the general shape of the two curves in Fig. 10 is similar demonstrates the consistency of the data and the analytical procedures. The FSDP is dramatically decreased by about 50% in amplitude after photodarkening. Other features at intermediate-q values also show certain changes. In general, the decreasing amplitudes with photodarkening indicate again, as do the total structure factors, that the structure overall moves to a more disordered state upon photoillumination. Considering the discussion in Sec. III A that the weighting factor of the As-S correlation at the two energies does not change much, we are led to the conclusion that the variation in structure by the photoillumination is dominated by the changing of the As-As atomic pair correlation.

C. The first sharp diffraction peak

The FSDP's at $q=1.1$ Å as shown in Fig. 6 represent the main evidence that there exists a certain IRO in these samples. The important issue involves any structure beyond the SRO which can contribute to the FSDP. This is: what is the origin of the FSDP? This has been a matter of controversy for a long time. Fowler and Elliot[54] in their computer modeling study suggested that the

FSDP is probably due to contributions of Fourier components from a broad region of real space, such as a density deficit at about 4.5 Å, rather than a distinct structural feature.

In this study, we use an inverse Fourier transform method as shown in Fig. 11 to increase our understanding of the origin of the FSDP. The reduced structure factor and the reduced radial distribution function are two equivalent expressions in two different spaces (i.e., q space and r space, respectively), if the scattering pattern beyond q maximum is not significant (i.e., if it is close to the structureless independent scattering factor) and if the radial distribution function beyond R maximum is close to the average atomic density. Therefore, to make inverse Fourier transforms, we fix the lower range of r at the origin and vary the upper limit of r. Any feature in a continuous scattering pattern arises from the linear superposition of many Fourier harmonics. The truncation of the r range is a simple removal of the components of the Fourier harmonics from the truncated range, although a termination error could be introduced into the inverse Fourier transforms. Figure 11 shows that the inverse Fourier transforms obtained in this way. From the bottom curve to the top, the r maximum changes from 10 to 7.68, 6.52, 6.11, 5.09, 3.89, and 3.24 Å. Comparing these curves, we can see the bottom two curves are very similar, suggesting that the structure beyond 7.68 Å in r space does not affect the scattering pattern significantly. In other words, the structure beyond 7.68 Å in this amorphous material is very close to the average atomic density, or structureless. The third curve from the bottom, which is taken with r maximum at 6.52 Å, shows a significant change, especially at the position of the FSDP or 1.1 $Å^{-1}$. In this case, the peak seen in the two bottom curves is almost gone. With further decrease of R maximum, the top four curves are changed, not only at the lower-q side, but also at the higher-q side. As we know, intensity features of a scattering pattern at low q reflect mainly longer-range orderings in r space. Therefore, what we can say in this inverse Fourier transform study is that the FSDP at 1.1 $Å^{-1}$ involves certain structural ordering extending as far as a feature in r space at around 7 Å. The atomic structure below 6.5 Å (which, of course, also affects the FSDP somewhat) is not significant enough to result in a FSDP as strong as that which is observed.

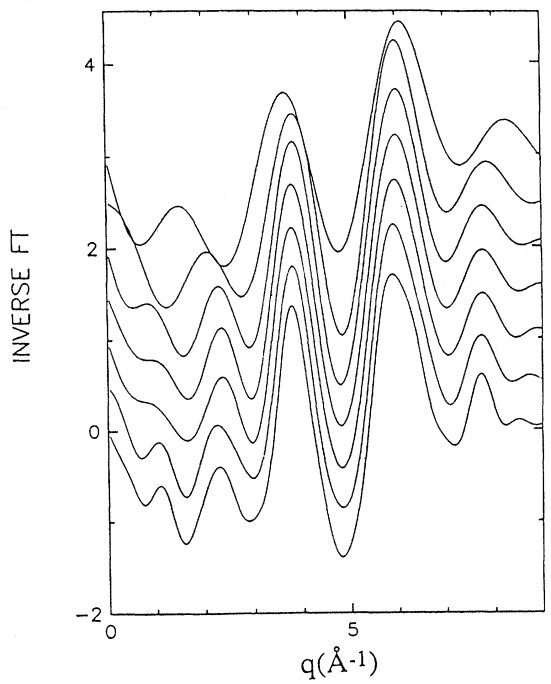

FIG. 11. Inverse Fourier transforms of the data in Fig. 9 vs q. The R minimum is taken at the origin. From the bottom line to the top, the R maximum is taken to be at 10, 7.68, 6.52, 6.11, 5.09, 3.89, and 3.24 Å.

It has been suggested by de Neufville, Moss, and Ovshinsky,[55] and applied by others,[56,57] that structural correlations in amorphous materials could be approximately determined by applying the Scherrer formula[58] to the FSDP. For the annealed sample of a-As_2S_3 measured at an x-ray wavelength $\lambda = 1.06$ Å ($E = 11\,700$ eV), the result is a length of 21 Å. But, the use of the Scherrer formula which is used to analyze the width of a diffraction peak containing many harmonics is not strictly applicable to a peak in the x-ray-scattering pattern which has, at most, a few harmonic components. This caveat was indeed recognized by de Neufville in the original paper[55] but apparently has not been recognized subsequently.

Many models have been proposed to associate with the scattering data, especially to identify the origin of the FSDP's. These include random helical segments,[59,60] "rafts,"[61] layered structure,[7,8,62] dense random packing,[10,11] etc. As we know, modeling plays an important role in structural studies of amorphous solids. The choice between possible models, in the case as presented in this paper which includes both structure and photoinduced structural changes, involves not only diffraction data but also a wide range of other techniques, such as vibrational and magnetic resonance spectroscopies. However, we do not discuss this issue in this paper any further. An extensive discussion by Zhou can be found elsewhere.[63]

V. CONCLUSIONS

Comparing the scattering data between the annealed and photodarkened a-As_2S_3 films, we conclude that the structure overall (both the SRO and the IRO) moves to a more disordered state upon photoillumination. The photoinduced structural changes involve the changes of the As-As atomic pair correlation. Study of the FSDP leads us to conclude that the FSDP is related to the intermediate-range correlations and these correlations are extended as far as 7.0 Å. Beyond 7.0 Å, however, the structure in radial distribution function in a-As_2S_3 tends to the average atomic density. Through the discussions of the total scattering factors at the two different x-ray

energies and their differentials, we conclude that the FSDP is dominated by the arsenic related atomic correlations, especially the As-As atomic correlation. Further measurements are planned to extend the q space range and improve the signal-to-noise ratio in order to attempt a quantitative analysis of the differential distribution function.

ACKNOWLEDGMENTS

We would like to thank Jean-Marc Tonnerre for the discussion about the experiment and to Mobil Co. for their financial support. This work in part is supported by U.S. Department of Energy, Division of Materials Sciences under Contract No. DE-FG05-89ER45384.

*Present address: Brookhaven National Laboratory, Building 801, Upton, NY 11973.

[1]P. C. Taylor, S. G. Bishop, and D. L. Mitchell, Solid State Commun. **8**, 1783 (1973).

[2]G. Lucovsky, Phys. Rev. B **6**, 1480 (1972).

[3]G. Lucovsky and R. M. Martin, J. Non-Cryst. Solids **8-10**, 185 (1972).

[4]S. G. Bishop and P. C. Taylor, Solid State Commun. **11**, 1323 (1972).

[5]R. J. Kobliska and S. A. Solin, J. Non-Cryst. Solids **8-10**, 191 (1972); Phys. Rev. B **8**, 756 (1973).

[6]A. J. Leadbetter and A. J. Apling, J. Non-Cryst Solids **15**, 250 (1974).

[7]L. E. Busse, Phys. Rev. B **29**, 3639 (1984).

[8]K. Tanaka, J. Non-Cryst. Solids **119**, 254 (1990).

[9]M. F. Daniel, A. J. Leadbetter, A. C. Wright, and R. N. Sinclair, J. Non-Cryst. Solids **32**, 271 (1979).

[10]S. C. Moss and D. L. Price, in *Physics of Disordered Materials,* edited by D. Adler, H. Fritzsche, and S. R. Ovshinsky (Plenum, New York, 1985), pp. 77–95.

[11]D. L. Price, S. C. Moss, R. Reijers, M.-L. Saboung, and S. Susman, J. Phys. C **21**, L1069 (1988).

[12]S. R. Elliott, T. Rayment, and S. Cummings, J. Phys. (Paris) Colloq. **43**, C9-35 (1982).

[13]D. G. Semak, V. I. Mikla, I. P. Mikhal'ko, V. A. Stefanovich, V. Yu. Slivka, and Yu. M. Vysochanskii, Fiz. Tverd. Tela (Leningrad) **26**, 3210 (1984) [Sov. Phys. Solid State **26**, 1934 (1984)].

[14]A. Fischer-Colbrie and P. H. Fouss, J. Non-Cryst. Solids **126**, 1 (1990).

[15]T. T. Penfold and P. S. Salmon, Phys. Rev. Lett. **67**, 97 (1991).

[16]H. Kawamura, F. Fukumasu, and Y. Hamada, Solid State Commun. **43**, 229 (1982).

[17]G. Pfeiffer, M. A. Paesler, and S. C. Argawal, J. Non-Cryst. Solids **130**, 111 (1991).

[18]Ka. Tanaka, J. Non-Cryst. Solids **35&36**, 1023 (1980).

[19]H. Hamanaka, K. Tanaka, A. Matsuda, and S. Iizima, Solid State Commun. **19**, 499 (1976).

[20]H. Hamanaka, K. Tanaka, and S. Iizima, Solid State Commun. **23**, 63 (1977).

[21]M. Frumar, A. P. Firth, and A. E. Owen, Philos. Mag. B **50**, 463 (1984).

[22]C. Y. Yang, M. A. Paesler, and D. E. Sayers, Phys. Rev. B **36**, 9160 (1987).

[23]W. Zhou, M. A. Paesler, and D. E. Sayers, Phys. Rev. B **46**, 3817 (1992).

[24]J. P. Lamagnac, J. Grenet, and P. Michon, Philos. Mag. B **45**, 627 (1982).

[25]B. T. Kolomiets, S. S. Lantratova, V. M. Lyubin, V. P. Pukch, and M. A. Tagirdzhanov, Fiz. Tverd. Tela (Leningrad) **18**, 1189 (1976).

[26]I. Janossy, J. Hajto, and W. K. Choi, J. Non-Cryst. Solids **90**, 529 (1987).

[27]V. M. Lyubin and V. M. Tikhomirov, J. Non-Cryst. Solids **114**, 133 (1989).

[28]K. Murayama, in *Disordered Semiconductors,* edited by M. A. Kastner, G. A. Thomas, and S. R. Ovshinsky (Plenum, New York, 1987), p. 185.

[29]J. M. Lee, M. A. Paesler, and D. E. Sayers, J. Non-Cryst. Solids **123**, 295 (1990).

[30]J. P. De Neufville, S. C. Moss, and S. R. Ovshinsky, J. Non-Cryst. Solids **13**, 191 (1973).

[31]W. Zhou, J. M. Lee, D. E. Sayers, and M. A. Paesler, J. Non-Cryst. Solids **114**, 43 (1989).

[32]I. L. Likholit, V. M. Lyubin, V. F. Masterov, and V. A. Fedorov, Fiz. Tverd. Tela **26**, 172 (1984) [Sov. Phys. Solid State **26**, 101 (1984)].

[33]P. J. Gaczi and H. Fritzsche, Solid State Commun. **38**, 23 (1981).

[34]J. Z. Liu and P. C. Taylor, Phys. Rev. B **41**, 3163 (1990).

[35]M. Rubinstein and P. C. Taylor, Phys. Rev. B **9**, 4258 (1974).

[36]D. J. Treacy, P. C. Taylor, and P. B. Klein, Solid State Commun. **32**, 423 (1979).

[37]J. Wells and P. Boolchand, J. Non-Cryst. Solids **89**, 31 (1987).

[38]S. S. Lantratova, V. M. Lyubin, and P. S. Seregin, Fiz. Tverd. Tela **25**, 2494 (1983) [Sov. Phys. Solid State **25**, 1432 (1983)].

[39]I. Zitkovsky and P. Boolchand, J. Non-Cryst. Solids **114**, 70 (1989).

[40]M. Iijima and Y. Mita, Solid State Commun. **24**, 665 (1977).

[41]P. J. S. Ewen, M. J. Sik, and A. E. Owen, Solid State Commun. **33**, 1067 (1980).

[42]S. A. Solin and G. N. Papatheodorou, Phys. Rev. B **15**, 2084 (1977).

[43]R. J. Nemanich, G. A. N. Connell, T. M. Hayes, and R. A. Street, Phys. Rev. B **12**, 6900 (1978).

[44]D. T. Cromer and J. B. Mann, Acta Crystallogr. A **42**, 321 (1968).

[45]M. S. Jensen, Phys. Lett. **74A**, 41 (1979).

[46]N. J. Shevick, Philos. Mag. **35**, 805 (1977).

[47]N. J. Shevick, Philos. Mag. **35**, 1289 (1977).

[48]P. H. Fuoss, P. Eisenberger, W. K. Warburton, and A. Bienenstock, Phys. Rev. Lett. **46**, 1537 (1981).

[49]G. Nicoli, R. Andouart, C. Barbier, D. Dagneaux, M. de Santis, and D. Raoux, in *Proceedings of the 2nd European Conference on Progress in X-Ray Synchrotron Radiation Research,* edited by A. Balerna, E. Bernieni, and S. Mobilio (STF, Bologna, 1990), p. 351.

[50]Jean-Marc Tonnerre, Ph.D. thesis, Universite de Paris-Sud, 1989.

[51]N. Norman, Acta Crystallogr. **10**, 370 (1957).

[52]D. T. Cromer and J. B. Mann, Acta Crystallogr. A **24**, 321 (1968).

[53]K. Tanaka, S. Iizima, K. Aoki, and S. Minomura, in *Proceedings of the 6th International Conference on Amorphous and Liquid Semiconductors,* edited by B. T. Kolomiets (Nauka, Moscow, 1976), p. 442.

[54]T. G. Fowler and S. R. Elliott, J. Non-Cryst. Solids **92**, 31 (1987).
[55]J. P. de Neufville, S. C. Moss, and S. R. Ovshinsky, J. Non-Cryst. Solids **13**, 191 (1973).
[56]R. J. Nemanich, Phys. Rev. B **16**, 1655 (1977).
[57]M. Essamet, B. Hepp, N. Proust, and J. Dixmier, J. Non-Cryst. Solids **97/98**, 191 (1987).
[58]H. R. Klug and L. E. Alexander, *X-Ray Diffraction Procedures* (Wiley, New York, 1974), p. 687.
[59]C. J. Brabec, Phys. Rev. B **44**, 13 332 (1991).
[60]L. Cervinka, J. Non-Cryst. Solids **106**, 291 (1988).
[61]J. C. Phillips, J. Non-Cryst. Solids **44**, 17 (1981).
[62]P. H. Gaskell, M. C. Eckersley, A. C. Barnes, and P. C. Chieux, Nature **350**, 675 (1991).
[63]W. Zhou, Ph.D. thesis, North Carolina State University, 1991 (unpublished).